Design, Construction, and Testing of 0.5-m, 18-mm Period Nb₃Sn Superconducting Undulator Magnets

I. Kesgin, M. Kasa, S. MacDonald, D. Turrioni, E. Barzi, Y. Shiroyanagi, Q. Hasse,
Y. Ivanyushenkov, A.V. Zlobin and E. Gluskin

Abstract— Design and fabrication of a new Nb₃Sn-based superconducting undulator (SCU) are underway at the Advanced Photon Source (APS) of Argonne National Laboratory in collaboration with Fermilab and Lawrence Berkeley National Laboratory. To develop a robust and reliable fabrication process, the magnet development consists of several steps. First, magnetic and mechanical simulations were performed to optimize the magnet design; then the design matured further by fabricating and testing a series of very short prototypes, ~8 cm long with a period length of 18 mm. These short prototype studies were previously reported. Second, the design was scaled to an intermediate length of ~0.5 m. These two steps led to the final design of ~1.1-m-long magnets, which are currently being fabricated. The quench behavior of each 0.5-m-long undulator magnet, as well as undulator assemblies from these magnets, was studied. The first SCU assembly did not meet the design specifications due to breakdown of the insulation. The second SCU assembly, with an improved design and fabrication process based on lessons learned, achieved the design undulator field of 1.2 T. The design was further optimized, and a third set of magnets was fabricated and successfully tested.

Index Terms—**Nb₃Sn, superconducting undulator, SCU, stability, magnet design, quench**

I. INTRODUCTION

SIGNIFICANT progress has been made in advancing Nb₃Sn undulator technology (SCU) in the past number of years [1-6]. These studies have revealed unresolved issues, and there are no operating Nb₃Sn-based SCUs at any light source facility to date. The Advanced Photon Source at Argonne National Laboratory has initiated a project with two main goals: to advance the Nb₃Sn-based SCU technology and to deliver a novel x-ray source to APS users.

Details on the scope of the project were published in our previous publications [7, 8]. Throughout these studies, the heat treatment cycle was optimized to improve stability of the Nb₃Sn wire [9, 10]. Mechanical simulations have been performed to calculate the deformation of the SCU magnets under high magnetic forces, and the magnet winding core design was optimized. Magnetic simulations have been conducted to optimize the winding groove dimensions, and an ideal winding configuration was chosen for the desired performance and convenient winding. Several short 4.5-period prototypes (18-mm period) were fabricated for these optimization studies [7, 11].

After the desired performance was confirmed, the design was scaled up to 26.5-period (28.5 with corrector magnets), ~0.5-m-long prototypes. Since the first two 0.5-m-long undulator magnets demonstrated weak insulation behavior, it drew some skepticism to the fabrication processes. To eliminate this negative perception and establish reliable fabrication steps, five more 0.5-m-long prototypes were fabricated. Several wire-to-ground insulation schemes were investigated, and the effect of the ground insulation choice on the SCU's magnet quench performance was analyzed. Details of the test results are presented in the following sections.

II. 0.5-M-LONG Nb₃Sn SUPERCONDUCTING UNDULATOR MAGNET FABRICATION

SCU magnets consist of cores. Each magnet core is made of a soft iron that has multiple grooves on its body to accommodate the superconducting wires [12-14]. The design undulator on-axis field is 1.2 T with a magnetic gap of 9.5 mm. The number of turns in a winding groove is 46. The Nb₃Sn wire is 0.6 mm RRP 146/169 braided with ~65-µm-thick fiberglass insulation. The non-copper fraction is ~48%. Further details on the Nb₃Sn undulator fabrication steps can be found in [7, 8, 11].

The fabricated undulator magnets were assembled with precise gap spacers located in three predefined locations along the length of the undulator magnet. Clamps were used at the same locations to provide mechanical rigidity and maintain gap uniformity (see Fig.1). Each magnet was equipped with a center voltage tap to allow monitoring of voltages from both halves of a magnet. This allowed determination of which half of the magnet quenches and can provide an idea about the uniformity. These two halves of the magnets are called "top" and "bot" referring to the top half and bottom half of the magnets when they placed inside the vertical test cryostat. After the assembly was completed, undulator magnets were inserted inside a vertical above-the-ground cryostat and pre-cooled to about 200 K with the liquid nitrogen in the cryostat outer jacket; then the liquid helium was transferred into the magnet space. The temperature of the magnets was monitored by two calibrated temperature

TABLE I
Nb₃Sn SCU SPECIFICATIONS OF 0.5-M-LONG UNDULATOR MAGNET

	IMM1	IMM2	IMM3	IMM4	IMM5	IMM6
Groove width (mm) before ground insulation	5.35	5.35	5.35	5.35	5.35	5.35
Machined groove width and depth (mm × mm)	5.55 × 4.8	5.55 × 4.8	5.65 × 4.9	5.65 × 4.9	5.65 × 4.9	5.65 × 4.9
Ground insulation	100 μm mica	100 μm mica	100 μm mica plus 100 μm Al₂O₃	100 μm mica plus 100 μm Al₂O₃	150 μm Al₂O₃	150 μm Al₂O₃
Short sample average RRR (RT to 19 K)	81	86	355	63	74	73
Sort sample limits, A	1200	1185	1200	1180	1170	1160

sensors located on the top and bottom of the magnets. Subsequently one after another, were individually trained at above the maximum design current, then in an undulator configuration. To detect a quench, the differential voltages from both halves of an undulator magnet or each magnet in an undulator configuration are compared to a set threshold, and the quench detection is activated.

A. Coil-to-Ground Insulation Selection

The very first short undulator prototypes were wound without any ground insulation under the assumption that the wire insulation would carry out this function. HiPot tests on the undulator magnets confirmed that the dielectric properties can withstand the maximum anticipated voltage in the event of a quench [11]. Nb₃Sn wire was insulated with ~65-micron-thick fiberglass braid—which is brittle and breaks easily during the winding—and coil-to-ground shorts formed in multiple spots. The winding process was repeated several times to eliminate these shorts, but they persisted. It was obvious that an additional ground insulation layer was needed. A 100-micron-thick mica was chosen as the main ground insulation. Mica was cut to the proper dimensions and placed inside the winding grooves before the undulator magnet winding. The addition of these mica structures made the winding process intolerant of any mistakes and sometimes resulted in insulation degradation in regions where the groove dimensions deviate from ideal. For this reason, the first 0.5-m-long prototype undulator magnets (IMM1

and IMM2; IMM stands for intermediate model magnet) suffered from an insulation damage [8]. It was clear that a more robust insulation scheme had to be developed and adopted.

Coating the undulator winding core with an Al₂O₃ plasma spray layer was implemented by LBNL as part of the SCU feasibility R&Ds for the free electron laser (FEL) [6], and this process was incorporated into the second set of 0.5-m-prototype magnets (IMM3 and IMM4) as shown in Fig. 1, top. To ensure redundancy, mica insulation was inserted between the Nb₃Sn wires and the Al₂O₃ layer. After winding the undulator magnet cores, they went through a heat treatment (HT) process at the Applied Physics and Superconducting Technology Division (APS-TD) of Fermilab and then epoxy impregnated at the APS. A picture of the magnet assembly is shown in Fig. 1, bottom.

To validate the robustness of the fabrication steps and further simplify the design, the mica insulation was eliminated in the third pair of undulator magnets (IMM5 and IMM6). One additional magnet (IMM7) in the same configuration was fabricated and is currently being tested. Table I provides a summary of the tested 0.5-m-long magnet parameters. One important conclusion to draw is that the measured average critical current limits and RRRs from the short samples are very close, which is an indication of a highly repeatable, well-controlled HT process. The RRR value of IMM3 is extraordinarily higher than the others. The origin of this behavior is currently unknown.

III. RESULTS AND DISCUSSIONS

Quench training profiles of six 0.5-m-long individual undulator magnets, in pairs, are shown in Fig. 2. Several short samples were included as part of the HT process and measured separately. The training quench currents are benchmarked to short sample limits (SSLs) in Fig. 2. The main difference between these magnet pairs is the choice of the ground insulation. The undulator magnets with only mica insulation (IMM1 and IMM2) demonstrated excellent quench training performance, which required only few quenches (<10) to reach the design current (Fig. 2, top). Very similar behavior was observed on the undulator magnets with the Al₂O₃ plasma spray layer plus mica (Fig. 2, middle). The performance of IMM5 and IMM6, where only the Al₂O₃ coating was used, showed an increase in the number of training quenches (Fig. 2, bottom). The likely explanation for this increase on the quench training could be the elimination of the mica as it reliefs the stresses [15]. The disadvantage of incorporating mica into the undulator design is that it complicates the winding. Because of this, the mica insulation

Fig. 1. Photographs of the undulator magnets after the Al₂O₃ plasma spray layer (top), and assembly in the undulator configuration (bottom).
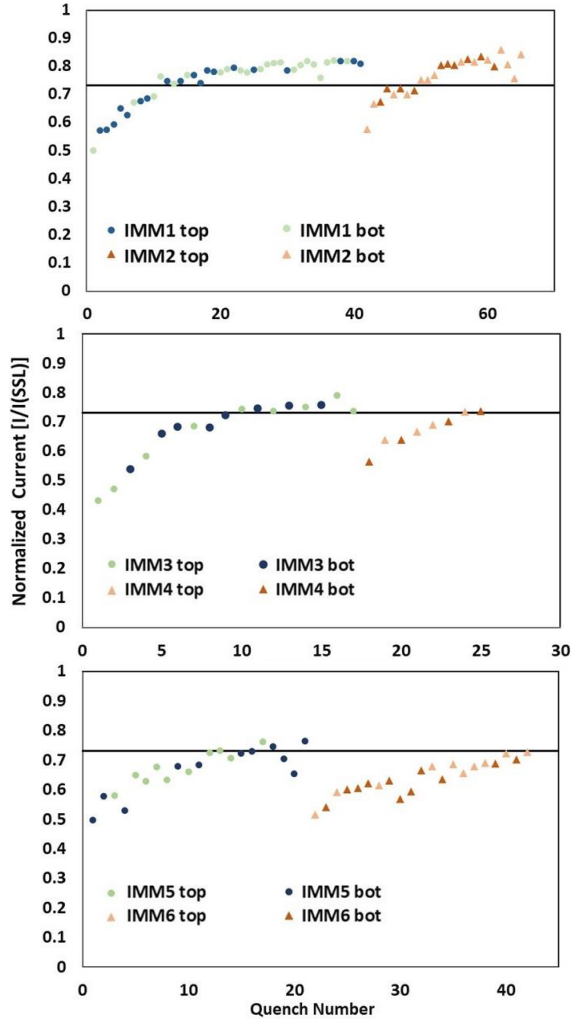
Fig 2. Training profiles of six 0.5-m-long undulator magnets up to the design current of 850 A (IMM1 to IMM6). The quench currents are normalized to short sample limits (SSLs). The maximum design current corresponds to ~73% of the SSLs.

was eliminated in the final 1.1-m-long undulator magnets in an expense to increase the number of training quenches. It is important to note that this final undulator magnet design is very modular, and in case the magnet training becomes a bottleneck, it is possible to incorporate the mica ground insulation with a very thin Al_2O_3 plasma spray layer.

Analysis of the distribution of the quenches displayed highly homogenous behavior across the magnet length (see Fig. 2). The number of quenches is almost the same in both halves of the magnets. These ensure that magnet fabrication steps do not introduce poor performing areas up to these current levels.

After characterizing the last undulator pair (IMM5 and IMM6), IMM6 was cooled down multiple times and trained. The normalized quench currents with respect to its SSL are shown in Fig. 3. It is important to note that this magnet has only Al_2O_3 ground insulation, and it requires extensive training to reach higher current levels. After about 100 quenches, the magnet reached 96% of its SSL with a remarkable current level of 1110A, which is only 50A lower than the SSL (1160A). This exercise proves that high current levels can be achieved in 0.5-

m-long undulator magnets albeit the fact that the amount of quench training is an issue that needs to be addressed by further design optimizations.

A. Quench Analysis

The maximum operational current density of a Nb_3Sn undulator is almost twice that of a similar NbTi undulator, which requires a robust and reliable quench detection and protection system. An active protection scheme (fabricated by LBNL) was implemented with an external dump resistor in series to a varistor (purchased from Metrosil, M&I Materials) to extract the stored energy from the Nb_3Sn undulator magnets. Understanding the quench behavior of the undulator magnets is a vital for their protections. Calculation of maximum hot spot temperature is widely used for this purpose. Under an adiabatic condition, the heat balance equation of unit volume of a winding can be written as

$$C(T)\frac{dT}{dt} = \rho_{Cu}(B,T)\frac{I^2(t)}{A_w A_{Cu}},\qquad(1)$$

where $C(T)$ is the volumetric specific heat of the winding and given by $C(T) = f_{Cu}C_{Cu}+(f_{Nb3Sn})C_{Nb3Sn}+(f_{G10})C_{G10}$. C_i and f_i are the temperature dependent volumetric specific heat and fraction of copper stabilizer, Nb_3Sn and insulation (G10). $\rho_{Cu}(B, T)$ is the temperature and magnetic-field-dependent copper resistivity; $I(t)$ is the quench current; A_w and A_{Cu} are the winding and Cu stabilizer cross sections, respectively. Integrating (1) from start to finish times (t_0 to t_{end}) is represented by

$$\int_{t0}^{tend}\frac{I^2(t)}{A_w A_{Cu}}dt = \int_{T_0}^{T_{max}}\frac{C(T)}{\rho_{Cu}(B,T)}dT,\qquad(2)$$

where T_{max} is the maximum hot spot temperature and can be calculated by integrating I^2 over the time span (t_0 to t_{end}) and using the temperature-dependent material properties. This approach is quite elegant as it does not depend on the size of the normal zone. Similar calculations can be performed by integrating $I{\cdot}V$ over the time span, and the quenched superconductor volume can be estimated. An example current decay profile from 850 A is provided in Fig. 5. Corresponding hot spot evolution, with 2-ms detection time, is also provided in the same figure. The current decay is not purely exponential and about 5-ms after the quench induced; the dynamic losses increase the coil internal resistance. Subsequently, the current decays faster
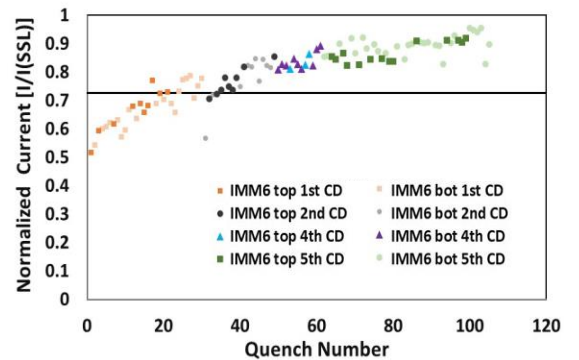
Fig. 3. Training profiles of IMM6 during multiple cooldown cycles. The magnet reached ~96% of its short sample limit after about 100 quenches. The maximum quench current is 1110A.
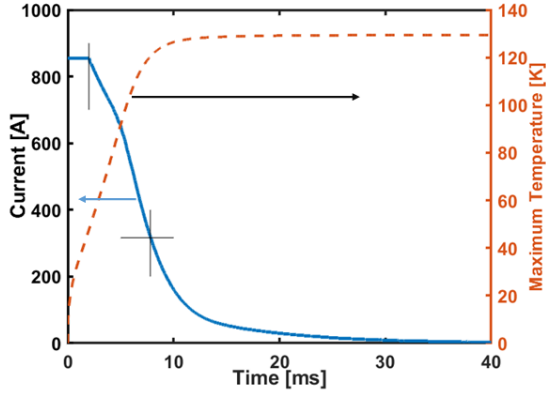
Fig 4. Hot spot temperature evolution during an artificially induced quench from 850 A with a 0.5 Ω dump resistor. The temperature growth and current decay with time are also shown. A 2-ms predetection time is included in the calculations. The decay constant is about 7.8 ms.

and a majority of the stored energy is deposited into the magnets from this point to the end of the quench event.

During testing of the magnets, the linear dump resistor value was adjusted to keep the maximum hot spot temperatures below the critical limit (~300 K). Hot spot temperatures calculated for an undulator pair using these current decay profiles with different dump resistor values and a varistor are provided in Fig. 5. These calculations include a 2-ms detection time. It is important to note that all these quenches are artificial, meaning that the current is kept at a certain value until the quench detection is manually triggered by lowering the threshold voltage. These calculations revealed that the undulator magnet design is robust and wide variety of linear resistance values can be used. One can use these calculations to adjust the final 1.1-m-long magnet linear resistance value. It is desirable to use as small a resistance value as possible, which would lower the maximum voltage and delay the contribution of the dynamic losses. This maximizes the extracted energy via the dump resistor and reduces the portion of the stored energy extracted by the undulator magnets; therefore, the pressure build-up in the cryostat becomes lower during the actual operation of the device, which accelerates the quench recovery process. However, one needs to pay special attention to keep the maximum hot spot temperature below the
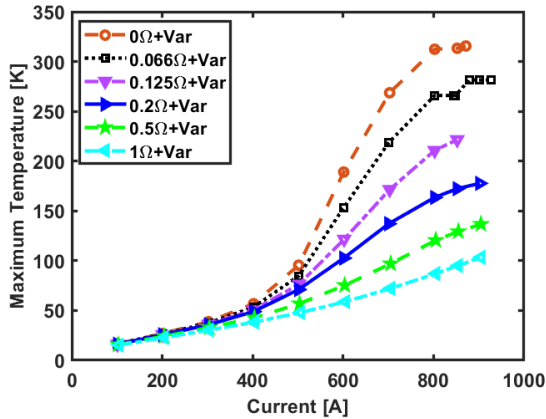
Fig. 5. Calculated hot spot temperatures for an undulator magnet pair from different current values using various linear resistor values in series to a varistor. The 2-ms quench detection time is included in the calculation of the maximum temperatures.
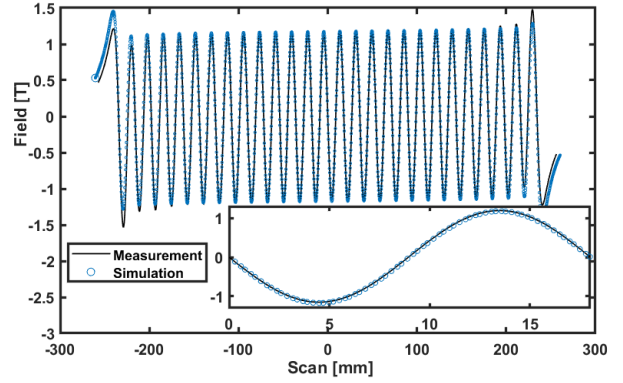
Fig 6. A field scan of a 0.5-m-long Nb$_3$Sn SCU. The Nb$_3$Sn SCU provides a 20% increase in the undulator field when compared to a similar NbTi SCU.

safe limit. Hot spot calculations using an adiabatic assumption is very conservative and can be safely used as a baseline for choosing the dump resistor value for protecting the final 1.1-m-long undulator magnets.

After completing training of the last magnet pairs (IMM5 and IMM6), the undulator fields were measured at the maximum operating current of 850A (Fig. 6) and compared with the 2D FEA simulations. These confirm the design field of ~1.2 T, and there is excellent agreement between the simulation and the measurement, as shown in the inset in the same figure.

IV. CONCLUSION

Seven 0.5-m-long Nb$_3$Sn SCU undulator magnet prototypes have been fabricated and tested. Five of them met design specifications requirements. Quench tests and detailed quench analyses have been performed to design and define the safe operation margin of the final 1.1-m-long magnets. Various ground insulation schemes were investigated, and the insulation choice was optimized. The design peak undulator field of 1.2 T at the maximum operating current of 850 A has been confirmed and agreed well with the simulations. Final Nb$_3$Sn undulator magnets are currently being fabricated, and once the assembly and characterization of the device is complete, the plan is to install it on the APS storage ring.

ACKNOWLEDGMENTS

REFERENCES

[1]   H. W. Weijers, K. R. Cantrell, A. V. Gavrilin, and J. R. Miller, "A Short-Period High-Field Nb$_3$Sn Undulator Study," *IEEE Transactions on Applied Superconductivity,* vol. 16, no. 2, pp. 311-314, 2006, doi: 10.1109/TASC.2006.870783.

[2]   H. W. Weijers, K. R. Cantrell, A. V. Gavrilin, E. L. Marks, and J. R. Miller, "Assembly Procedures for a Nb$_3$Sn Undulator Demonstration Magnet," *IEEE Transactions on Applied Superconductivity,* vol. 17, no. 2, pp. 1239-1242, 2007, doi: 10.1109/TASC.2007.899988.

[3]   S. Prestemon *et al.*, "Design and evaluation of a short period Nb$_3$Sn superconducting undulator prototype," in *Particle Accelerator Conference, 2003. PAC 2003. Proceedings of the*, 12-16 May 2003, vol. 2, pp. 1032-1034, 2003 doi: 10.1109/PAC.2003.1289595.

[4]   S. H. Kim, C. L. Doose, R. L. Kustom, and E. R. Moog, "Development of Short-Period Nb$_3$Sn Superconducting Undulators for the APS," *IEEE Transactions on Applied Superconductivity,* vol. 18, no. 2, pp. 431-434, 2008, doi: 10.1109/TASC.2008.920528.

[5]   D. R. Dietderich *et al.*, "Fabrication of a Short-Period Nb$_3$Sn Superconducting Undulator," *IEEE Transactions on Applied Superconductivity,* vol. 17, no. 2, pp. 1243-1246, 2007, doi: 10.1109/TASC.2007.897747.

[6]   D. Arbelaez *et al.*, "Superconducting Undulator Developments at Lawrence Berkeley National Laboratory," in International Committee for Future Accelerators, Beam Dynamics Newsletter No. 78, pp. 74-85, Editor J. Byrd, Argonne National Laboratory, Editor in Chief I. Hofmann, GSI/TUD, December 2019.

[7]   I. Kesgin *et al.*, "Fabrication and Testing of 10-Pole Short-Period Nb3Sn Superconducting Undulator Magnets," *IEEE Transactions on Applied Superconductivity,* vol. 30, no. 4, pp. 1-5, 2020, doi: 10.1109/TASC.2020.2964193.

[8]   I. Kesgin *et al.*, "Fabrication and Testing of 18-mm-Period, 0.5 m Long Nb$_3$Sn Superconducting Undulator," *IEEE Transactions on Applied Superconductivity,* pp. 1-1, 2021, doi: 10.1109/TASC.2021.3057846.

[9]   A. V. Zlobin, E. Barzi, D. Turrinoni, Y. Ivanyushenkov, and I. Kesgin, "Advantage and Challenges of Nb$_3$Sn Superconducting Undulators," presented at the 9th International Particle Accelerator Conference, Vancouver, BC, Canada, 04/29-05/04/2018, 2018.

[10] E. Barzi, M. Kasa, I. Kesgin, D. Turrioni, and A. V. Zlobin, "Heat threatment studies of Nb$_3$Sn wire for supeconducting planar undulators," *IEEE Transactions on Applied Superconductivity,* vol. Submitted, 2020.

[11] I. Kesgin *et al.*, "Development of Short-Period Nb$_3$Sn Superconducting Planar Undulators," *IEEE Transactions on Applied Superconductivity,* vol. 29, no. 5, pp. 1-4, 2019, doi: 10.1109/TASC.2019.2897645.

[12] I. Kesgin, M. Kasa, Y. Ivanyushenkov, and U. Welp, "High-temperature superconducting undulator magnets," *Superconductor Science and Technology,* vol. 30, no. 4, p. 04LT01, 2017, doi: 10.1088/1361-6668/aa5d48.

[13] Y. Ivanyushenkov *et al.*, "Status of the Development of Superconducting Undulators at the Advanced Photon Source," *Synchrotron Radiation News,* vol. 31, no. 3, pp. 29-34, 2018/05/04 2018, doi: 10.1080/08940886.2018.1460172.

[14] Y. Ivanyushenkov *et al.*, "Development and operating experience of a 1.1-m-long superconducting undulator at the Advanced Photon Source," *Physical Review Accelerators and Beams,* vol. 20, no. 10, p. 100701, 10/03/ 2017, doi: 10.1103/PhysRevAccelBeams.20.100701.

[15] N. Diaczenko *et al.*, "Stress management in high-field dipoles," in *Proceedings of the 1997 Particle Accelerator Conference (Cat. No.97CH36167)*, 16-16 May 1997 1997, vol. 3, pp. 3443-3445 vol.3, doi: 10.1109/PAC.1997.753236.